Int. J. Electrochem. Sci., 15 **(2020)** 2839 – 2850, doi: 10.20964/2020.03.29

International Journal of
ELECTROCHEMICAL
SCIENCE
www.electrochemsci.org

Evaluation of sulfur poisoning and carbon deposition on Co-infiltrated SOFCs $La_{0.4}Sr_{0.6}TiO_3$−$Gd_{0.2}Ce_{0.8}O_{1.9}$ Composite Anodes

Liquan Fan[1,*], *Tao Cong*[1], *Xinyu Su*[1], *Qianjun Hu*[2], *Yuwei Wang*[1], *Xiaotian Liu*[3],
Yufeng Li[1], *Hongge Jia*[1], *Yueping Xiong*[2,*]

[1] College of Materials Science and Engineering, Heilongjiang Provincial Key Laboratory of Polymeric Composite Materials, Qiqihar University, No.42, Wenhua Street, Qiqihar 161006, PR China
[2] School of Chemistry and Chemical Engineering, Harbin Institute of Technology, 92 West Dazhi Street, Harbin 150001, PR China
[3] Space Institute of Southern China, Shenzhen, 518117, PR China. Harbin Institute of Technology Shenzhen Graduate School, Shenzhen, 518055, PR China
[*]E-mail: Liquan_Fan@163.com; ypxiong@hit.edu.cn

Received: 20 October 2019 / *Accepted:* 16 December 2019 / *Published:* 10 February 2020

This paper presents H_2S and CH_4 tolerance of Co or Ni infiltration into porous nanofiber-based $La_{0.4}Sr_{0.6}TiO_3$−$Gd_{0.2}Ce_{0.8}O_{1.9}$ (LST−GDC) on yttria stabilized zirconia (YSZ) electrolyte disks. Over long-term stability tests performed on the nanofiber-based LST−GDC−Ni and LST−GDC−Co composite anodes in 512 ppm H_2S-H_2 (i.e. 512 ppm H_2S in H_2 atmosphere), the electrochemical performance and the porosity of the LST−GDC−Ni composite anode evolve to reduce significantly. Whereas, the LST−GDC−Co composite anodes exhibit a strong resistance to sulfur poisoning and then when exposed to humidified CH_4, show a good electrochemical performance, and the polarization resistance (R_p) of 2.96 Ω cm^2 and the maximum power density (P_{max}) of 53.7 mW cm^{-2} are achieved at 800 °C. The LST−GDC−Co composite anodes demonstrate excellent long-term stability and outstanding resistance to carbon deposition. The LST−GDC−Co composite anodes are a promising electrode material for sulfur-resistant and carbon tolerant solid oxide fuel cells.

Keywords: Carbon Deposition; Cobalt; Fuel Cell; Nanofiber-based Composite Anode; Sulfur Poisoning

1. INTRODUCTION

Solid oxide fuel cell (SOFCs) are an clean and efficient electrochemical energy conversion device with the advantages of environmental friendliness and fuel universality, which has attracted extensive attention and developed rapidly in recent years. Compared with other fuel cells, a SOFC tends to integrate with. industrial feedstock gases such as natural gas, coal gas and syngas and obtain ideal clean energy[1–3]. However, these carbon-based fuels can severely threaten the electrode performance of the conventional Ni-based anodes, such as Ni in Ni-YSZ composite anodes plays a role as a kind of catalysis and demonstrates high catalytic activity for hydrocarbon fuels. The deposited carbon covers the catalytic activity sites. In addition, sulfur-containing compounds such as H_2S are common impurities in the above gases, and these impurities can react with the conventional Ni-based anodes to form nickel sulfide with low catalytic activity to fuels[4–6]. The activity energy of H_2S decomposition on the Ni surface is low, and sulfur atoms are easily produced to occupy the activity sites of the Ni surface and then restrain fuel oxidation, even if relatively low H_2S content can evidently deteriorate the cell performance[7,8]. Thus, nickel-free mixed ionic-electronic conductor oxides such as perovskite with remarkable redox stability have been widely investigated as a kind of SOFC anode in recent years. $La_xSr_{1-x}TiO_3$-based anodes are viewed as a promising alternative anode for SOFCs[9–11], and when fed with sulfur-containing fuels exhibit good electrochemical performance and long-term stability, such as $La_{0.4}Sr_{0.6}TiO_{3\pm\delta}-Y_{0.2}Ce_{0.8}O_{2-\delta}$[12], cobalt doped $LaSrTiO_{3-\delta}$[13] and $La_{1-x}Sr_xBO_3$/8YSZ (B=Mn, Cr, Ti)[14]. In a previous study[15], it has been shown that the nanofiber-based LST−GDC−Ni composite anodes fabricated by infiltrating GDC and Ni into porous LST nanofiber backbones exhibit prominent electrochemical performance and long-term, thermal cycling and redox cycling stability when fueled with humidified hydrogen or humidified methane. However, even trace amount of sulfur-containing impurities in fuels could react with the Ni impregnation phase of LST−GDC−Ni, leading to severe performance degradation. Cobalt-based materials are a kind of widely used catalysts with excellent electrocatalytic activity[16] and sulfur poisoning resistance[13], which can be used in lots of hydrogen-related reactions[17,18]. Thus, infiltrating cobalt into the nanofiber-based LST−GDC composite anodes, considering the limitation of the nickel cermet anodes, can improve their resistance to sulfur poisoning effectively.

This article examines and compares resistance to sulfur poisoning of the nanofiber-based LST−GDC−Ni and LST−GDC−Co composite anodes. The electrochemical performance and long-term stability of LST−GDC−Co after sulfur tolerant tests are also investigated using humidified CH_4 as fuel. Furthermore, the microstructure of the LST−GDC−Ni and LST−GDC−Co composite anodes after tests has been studied.

2. EXPERIMENTAL

2.1. Cell fabrication

8 mol% Y_2O_3-92 mol% ZrO_2 (YSZ) electrolyte disks were prepared by cold isostatic pressing commercial YSZ (Huaqing Energy Technology Co., Ltd.) powders, followed by calcining in air at 1550 °C for 10 h. The electrolyte disks were about 19 mm in diameter and about 0.6 mm in thickness.

$La_{0.4}Sr_{0.6}TiO_3$ (LST) nanofibers were synthesized by electrospinning method. Appropriate amounts of polyvinylpyrrolidone (PVP) and concentrated nitric acid were dissolved into N,N-dimethylformamide (DMF) at room temperature under stirring until the solution became clear. And then stoichiometric amounts of lanthanum nitrate ($La(NO_3)_3\cdot 6H_2O$), strontium nitrate ($Sr(NO_3)_2$) and tetrabutyl titanate ($[CH_3(CH_2)_3O]_4Ti$) with molar ratios of 0.4:0.6:1 were added into the above solution, stirring for 12 h to obtain a homogeneous precursor solution of 9 wt.% PVP and 12 wt.% metal salts for electrospinning. The precursor solution was loaded into a plastic syringe equipped with a flat stainless steel needle of 0.8 mm in diameter. The distance between nickel mesh collector and the stainless steel needle was 12 cm, and the high voltage supply was set at 22 kV. The as-electrospun LST precursor nanofibers were calcined in air at 900 °C for 2 h.

Stoichiometric amounts of $Ce(NO_3)_3·6H_2O$ and $Gd(NO_3)_3·6H_2O$ were dissolved into the glycine solution (solvent was 50 vol.% ethyl alcohol and 50 vol.% deionized water) to form the impregnation precursor solution of 0.25 mol L^{-1} GDC. The molar ratio of metal cations and glycine in the solution was 2:3. $Ni(NO_3)_2·6H_2O$ was dissolved into deionized water to form the Ni impregnation precursor solution with 0.25 mol L^{-1} aqueous solution of nickel nitrate. Similarly, $Co(NO_3)_2·6H_2O$ was dissolved into deionized water to form the Co impregnation precursor solution with 0.25 mol L^{-1} cobalt nitrate.

The LST nanofibers were mixed with the terpineol solution which dissolved 3 wt.% ethylcellulose to form the anode slurry in 1:1 mass ratio of LST to terpineol solution. And then the anode slurry was coated as a spot (diameter was 10 mm) onto the YSZ electrolyte disks and sintered in air at 900 °C for 2 h, forming a LST nanofiber scaffold with a diameter of 10 mm. And so the effective area of the working electrode was 0.785 cm^2. The counter electrode (i.e. cathode) and the reference electrode were platinum and more details on the fabrication procedure has been explained in detail elsewhere[10]. The GDC impregnation precursor solution was infiltrated into the LST anode scaffold, and calcining in air at 800 °C for 1 h to prepare LST−GDC composite anodes. Then impregnating Ni or Co impregnation precursor solution into the LST−GDC composite anodes and calcining in air at 800 °C for 1 h, the single cells with the nanofiber-based LST−GDC−Ni and LST−GDC−Co composite anodes were fabricated successfully. Pt cathode, YSZ electrolyte and LST−GDC−Co (or LST−GDC−Ni) composite anode constituted a SOFC single cell.

2.2 Cell test and characterization

The anode current collector was Au mesh, and the cathode current collector was Pt mesh. All electrochemical measures was studied by an electrochemical workstation (CHI 650D, Shanghai CH Instruments Co., China). The LST−GDC−Ni or LST−GDC−Co were reduced for 4 h by H_2 at 800 °C before electrochemical tests. We tested the single cells using a self-made SOFC testing tube furnace. The cathode part was pumped with air while the anode was exposed to different atmospheres of humidified H_2 ($97\%H_2+3\%H_2O$), 512 ppm H_2S-H_2 and humidified CH_4 ($97\%CH_4+3\%H_2O$). Impedance measurements of the LST−GDC−Ni or LST−GDC−Co were carried out under open circuit voltage (OCV) over a frequency ranged from 0.1 Hz to 10 kHz with a 10 mV ac amplitude at 800 °C. An equivalent circuit of $LR_0(R_1Q)(R_2Q)$ was used for fitting to deconvolute the polarization[9–11,19], and L means inductance, Q stands for a constant phase element, R_0 represents ohmic resistance, R_1 represents high frequency region resistance (charge transfer process) and R_2 represents low frequency region resistance (surface diffusion and electrochemical reaction, surface adsorption/desorption). The sum of R_1 and R_2 is equal to the interface polarization resistance (R_p). The current−voltage (I−V) and current−power density (*I*−*P*) characteristics of the single cell consisting of LST−GDC−Ni or LST−GDC−Co composite anode, YSZ electrolyte and Pt cathode were also measured by the electrochemical workstation.

In the present work, a comparative study of the long-term stability tests of Ni- and Co-infiltrating LST−GDC was conducted at 800 °C. The composite anodes were loaded a constant voltage of 0.54 V and fueled with 512 ppm H_2S-H_2 for 24 h, the corresponding current density change was recorded. As for LST−GDC−Co, the fuel was then switched into humidified CH_4 after the sulfur poisoning test under a constant voltage of 0.56 V for 100 h, the corresponding current density change was recorded.

To compare the microstructure and phase formation before and after cell tests, the cross-sectional microstructures of LST−GDC−Ni and LST−GDC−Co before and after electrochemical testing were observed by a ZEISS SUPRA55 SAPPHIRE scanning electron microscope (SEM), and the phase analysis was performed on the composite anodes with a Bruker D8 Advance X-ray diffractometer (XRD) using a Cu-Kα radiation.

3. RESULTS AND DISCUSSION

Remarkable electrochemical performance and stability of the nanofiber-based LST−GDC−Ni composite anodes have been reported using humidified hydrogen or methane as fuel[15]. In order to explore sulfur tolerance of the nanofiber-based LST−GDC−Ni composite anodes, a long-term stability test of the LST−GDC−Ni with a mass ratio of LST:GDC:NiO=1:1:0.1 fueled with 512 ppm H_2S-H_2 was executed for a period of 21 h at 800 °C. The corresponding current density variation with time for the composite anode under a constant voltage of -0.54 V is depicted in Fig. 1. After reducing the LST−GDC−Ni composite anode under dry H_2, the reducing atmosphere was replaced by 512 ppm H_2S-H_2, the corresponding current density remained relatively steady during the first 1.5 h followed by the rise in instability in the next 2.2 h owing to the activation of nickel nanoparticles[15] combined with H_2S-induced enhancement[13]. Whereafter, a significant decrease in current density was observed and it continued for about 6 h. And from then it declined gradually until tended to be stable. The performance degradation was due to the poisoning effect of sulphur on the nickel nanoparticles, the resulting nickel sulfide has a poor electrocatalytic activity on fuels[5,20]. To compare the electrochemical performance before and after the sulfur poisoning testing for 21 h, impedance measurements were carried out. Electrochemical impedance spectroscopy (EIS) and the fitting results of the LST−GDC−Ni composite anode using 512 ppm H_2S-H_2 as fuel before and after sulphur poisoning at 800 °C are shown in Fig. 2. Impedance spectra of the LST−GDC−Ni composite anode appeared as two depressed capacitive arcs, which can be fitted by the equivalent circuit of $LR_0(R_1Q)(R_2Q)$[11,15]. The measured R_p values before and after the sulphur poisoning were 1.91 $\Omega\ cm^2$ and 4.04 $\Omega\ cm^2$, respectively. At the same time, the achieved maximum power density (P_{max}) decreased from 77.6 $mW\ cm^{-2}$ to 52.2 $mW\ cm^{-2}$, as shown in Fig. 3. These changes in electrochemical performance is likely due to the interaction of H_2S in fuel and Ni in the composite anode to produce nickel sulfide with deactivation to fuel and the resultant Ni phase coarsening caused by agglomeration[4–6]. To cast light on this, the cross-section SEM images of the LST−GDC−Ni composite anode before and after the sulfur poisoning test were compared, as shown in

Fig. 4. As observed, the porosity of the composite anode after sulfur poisoning decreases noticeably, since sulfur contamination lower the efficient surface of Ni nanoparticles introduced by infiltration, leading to a decrease in the three-phase boundary (TPB) region of the electrode which could severely degrade cell performance[21]. Hu et al.[15] demonstrated that the porosity and microstructure of the nanofiber-based LST−GDC−Ni composite anode under humidified H_2 for 2700 min did not change significantly.

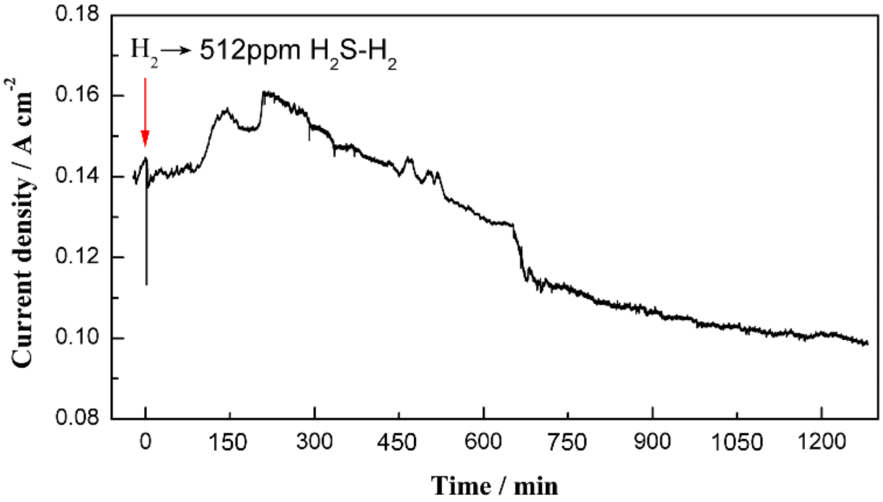

Figure 1. Current density variation with time for the LST−GDC−Ni composite anode under a constant voltage of -0.54 V. After reducing the LST−GDC−Ni composite anode under dry H_2, start the time when the reducing atmosphere was replaced by 512 ppm H_2S-H_2.

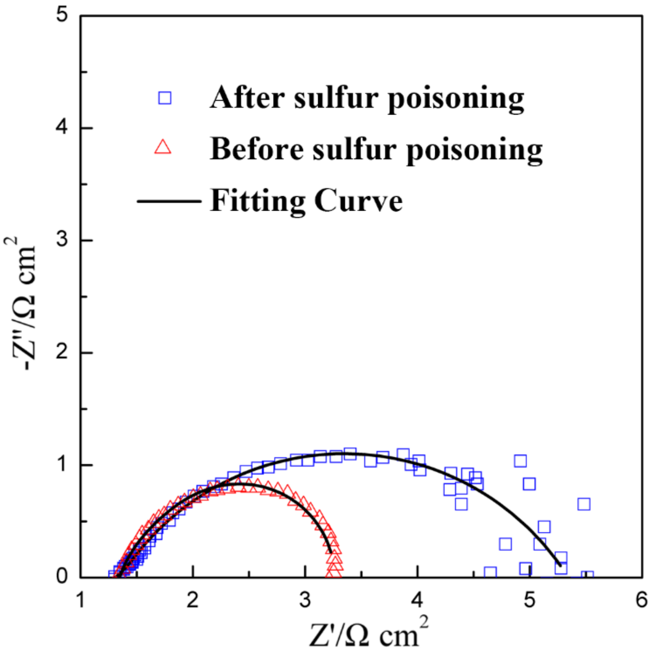

Figure 2. Impedance spectra of the LST−GDC−Ni composite anode before and after sulfur poisoning testing under 512 ppm H_2S-H_2 at 800 °C.

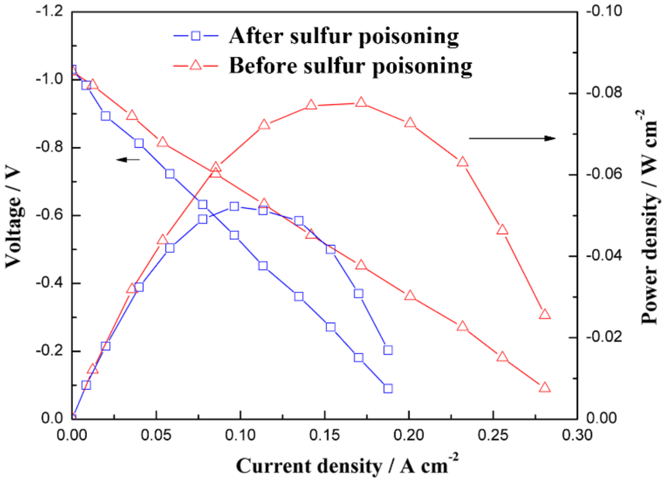

Figure 3. *I*−*V* and *I*−*P* characteristics for the single cell consisting of LST−GDC−Ni composite anode, YSZ electrolyte and Pt cathode tested at 800 °C. 512 ppm H_2S-H_2 was on the anode side and air was on the cathode side.

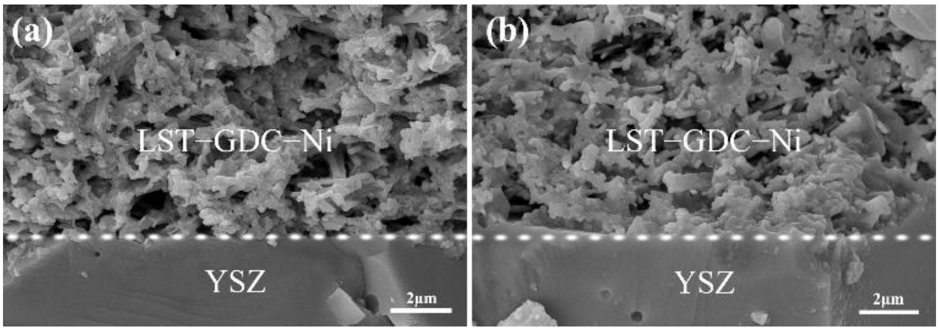

Figure 4. Cross-section SEM images of the LST−GDC−Ni composite anode before (a) and after (b) sulfur poisoning.

Comparison between the results reasonably supports the abovementioned argument that the H_2S impurity in fuel gas poisoned and agglomerated the Ni nanoparticles of the composite anode, leading to the lower porosity and smaller TPB area, and so the electrochemical performance degraded obviously after sulfur poisoning. Thus, the nanofiber-based LST−GDC−Ni composite anode had poor endurance to sulfur poisoning.

Cobalt-based catalysts are widely used for its excellent electrocatalytic activity[16] and sulfur poisoning resistance[13] in SOFC electrodes. As an alternative to the nickel impregnation phase, we infiltrated Co impregnation precursor solution into the nanofiber-based LST−GDC composite anodes to prepare the nanofiber-based LST−GDC−Co composite anode. Fig. 5 shows the XRD patterns of the LST−GDC−Co composite anode on YSZ electrolyte before and after reduction under humidified H_2 (97%H_2+3%H_2O) for 4 h at 800 °C. The measured XRD pattern of YSZ (Huaqing Energy Technology Co., Ltd.) and the standard XRD patterns of LST (PDF#79-0188), GDC (PDF#75-0162), Co_3O_4 (PDF#74-2120) and Co (PDF#15-0806) are also given as guides to the eyes at the bottom of Fig. 5. After reduction, all the diffraction peaks were indexed to LST, GDC, Co and YSZ. Besides, no impurity diffraction peak was present. This clearly indicates Co_3O_4 was reduced to Co after reduction for 4 h and the nanofiber-based LST−GDC−Co composite anodes were fabricated successfully.

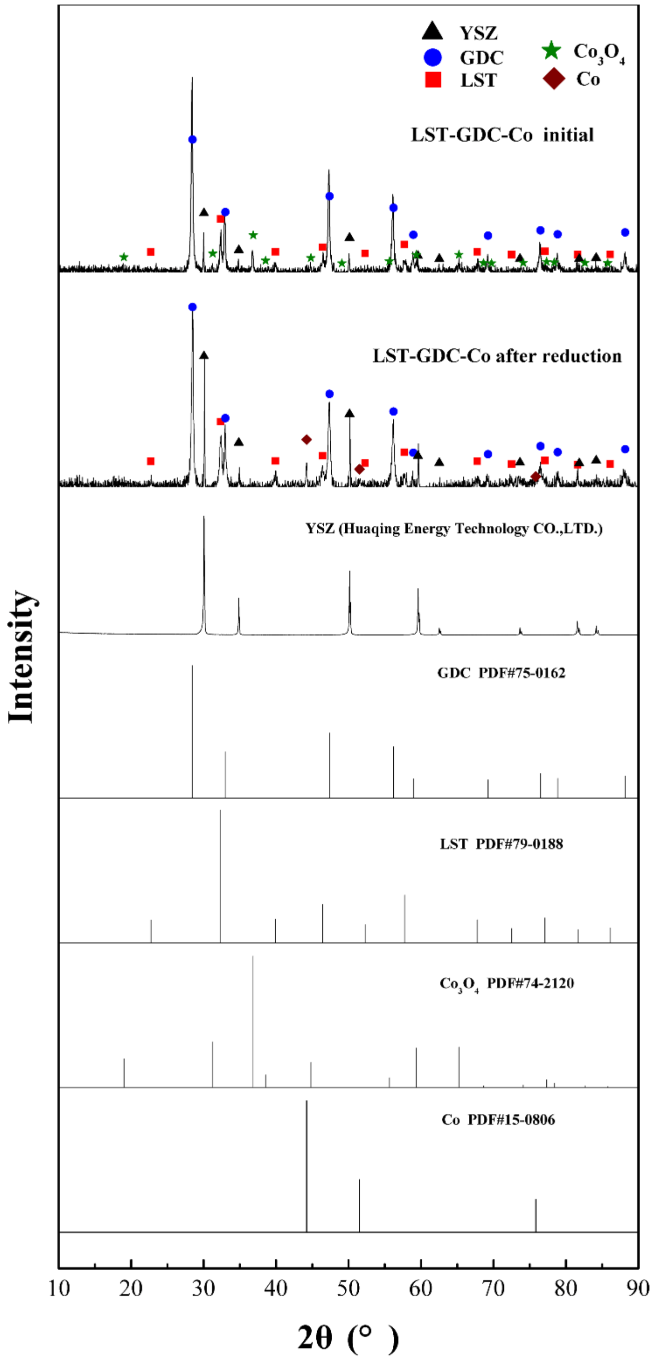

Figure 5. XRD pattern of the LST−GDC−Ni composite anode on YSZ electrolyte. The measured XRD pattern of YSZ (Huaqing Energy Technology Co., Ltd.) and the standard XRD patterns of LST (JCPDS card no. 79-0188), GDC (JCPDS card no. 75-0162), Co_3O_4 (JCPDS card no. 74-2120) and Co (JCPDS card no. 15-0806) are given as references at the bottom.

For the sake of exploring sulfur tolerance and carbon deposition resistance of the nanofiber-based LST−GDC−Co composite anodes, a long-term stability test of LST−GDC−Co with mass ratio of LST:GDC: Co_3O_4=1:1:0.3 was conducted at 800 °C according to the profile as shown in Fig. 6(a). The detailed process was as follow: (1) The air was replaced by humidified (3% H_2O) Ar gas in the anode, a sudden jump in the potential was observed. After 1 h, the open circuit potential (OCP) was found to be about -0.15 V. The anode atmosphere was changed from humidified Ar gas to 97%H_2+3%H_2O mixture gas and kept for up to 4 h. A polarization resistance test of the anode (marked with R_p-H_2-1) and *I*−*V* and *I*−*P* test of the single cell (marked with P-H_2-1) were carried out; (2) The 97%H_2+3%H_2O mixture gas was switched into 97%CH_4+3%H_2O. A polarization resistance test of the anode (marked with R_p-CH_4-1) and *I*−*V* and *I*−*P* test of the single cell (marked with *P*-CH_4-1) were done after keeping in 97%CH_4+3%H_2O for 1 h; (3) The anode atmosphere was changed into 512 ppm H_2S-H_2 and kept for 1 h. Subsequently, a constant voltage of 0.54 V under open circuit condition was loaded on the single cell for a period of 24 h, the corresponding current density variation with time is depicted in Fig. 6(b).

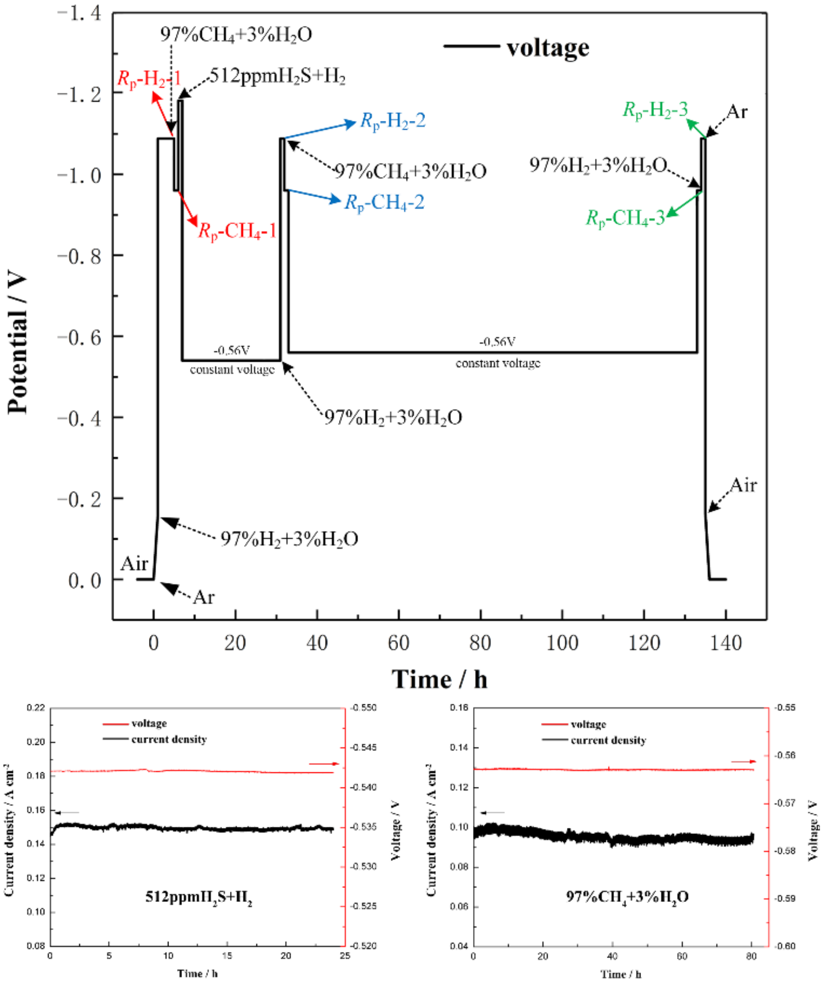

Figure 6. (a) Long-term stability test profile of the LST−GDC−Co composite anode at 800 °C. The corresponding current density variation with time for the anode fueled with 512 ppm H_2S-H_2 under a constant voltage of 0.54 V for 24 h (b) and humidified CH_4 (97%CH_4+3%H_2O) under a constant voltage of 0.56 V for 100 h (c) at 800 °C.

The fuel at the anode side was converted into 97%H_2+3%H_2O and remained for 1 h, followed by AC impedance and *I*−*V* and *I*−*P* measurements (marked as R_p-H_2-2 and *P*-H_2-2, respectively); (4) The anode part was pumped with 97%CH_4+3%H_2O instead of 97%H_2+3%H_2O. After 1 h, a polarization resistance test of the anode (marked with R_p-CH_4-2) and *I*−*V* and *I*−*P* test of the single cell (marked with *P*-CH_4-2) were executed. (5) A constant voltage of 0.56 V under OCP condition was loaded on the single cell for 100 h, the corresponding current density change with time is plotted in Fig. 6(c). After stopping the constant voltage for 1 h, a polarization resistance test of the anode (marked with R_p-CH_4-3) and *I*−*V* and *I*−*P* test of the single cell (marked with P-CH_4-3) were done. The anode atmosphere was changed from 97%CH_4+3%H_2O to 97%H_2+3%H_2O and kept for 1 h. A polarization resistance test of the anode (marked with R_p-H_2-3) and *I*−*V* and *I*−*P* test of the single cell (marked with P-H_2-3) were carried out. (6) The anode atmosphere was changed into humidified Ar gas, the measured OCP after 1 h was about -0.15 V. The humidified Ar gas was switched off, air was then introduced into the anode side. As seen from Fig. 6(b) and (c), the current density didn't take place obvious change and no degradation occurred. This result suggests that the nanofiber-based LST−GDC−Co composite anodes have excellent long-term stability in 512 ppm H_2S+H_2 or 97%CH_4+3%H_2O mixture gas.

During the abovementioned period of long-term stability test, all of the impedance measurements and the *I*−*V* and *I*−*P* characteristics before and after sulfur poisoning or carbon deposition are comparatively exhibited in Fig. 7. The obtained R_p values and the maximum power density (P_{max}) values when anode fueled with humidified H_2 or CH_4 are summarized in Table 1. When using humidified H_2 as fuel, the R_p value of the LST−GDC−Co after reduction for 4 h (R_p-H_2-1) was 0.48 Ω cm^2, which was slightly lower than that of the LST−GDC−Ni reported by Hu et al. (R_p=0.52 Ω cm^2)[15] under the same measurement condition. The R_p value (R_p-H_2-2) increased slightly up to 0.59 Ω cm^2 after sulfur poisoning test under 512 ppm H_2S-H_2 atmosphere for a period of 24 h, however, it is still obviously lower than those of the nanofiber-based LST−GDC composite anodes without Co infiltration phase (1.73 Ω cm^2 and 1.31 Ω cm^2 for the LST−GDC (1:1) and LST−GDC (1:1.3), respectively)[11]. When the fuel switched into humidified CH_4, the R_p value (R_p-CH_4-1) was 1.97 Ω cm^2 and the P_{max} value (P-CH_4-1) was 71.3 mW cm^{-2}. After sulfur poisoning for 24 h, the R_p value (R_p-CH_4-2) increased obviously to 2.96 Ω cm^2,which is close to the value for the LST−GDC−Ni without sulfur poisoning (2.86 Ω cm^2), the P_{max} value (*P*-CH_4-2) decreased to 53.7 mW cm^{-2} which is higher than that of the nanofiber-based LST−GDC composite anode (3.9 mW cm^{-2})[15]. Co nanoparticles of the composite anode reacted with H_2S and formed cobalt sulfide at 512 ppm H_2S-H_2 atmosphere, which has good catalytic activity on humidified CH_4[22,23]. After carbon deposition test for 100 h, the R_p value and the maximum power density at humidified H_2 or CH_4 atmosphere fluctuated slightly, we did not find the obvious change of the LST−GDC−Co electrochemical performance. Thus, we could conclude that the nanofiber-based LST−GDC−Co composite anode had good resistance to sulfur poisoning, and the LST−GDC−Co after sulfur poisoning showed excellent electrochemical performance when fueled with humidified methane and an excellent carbon depositing resistance.

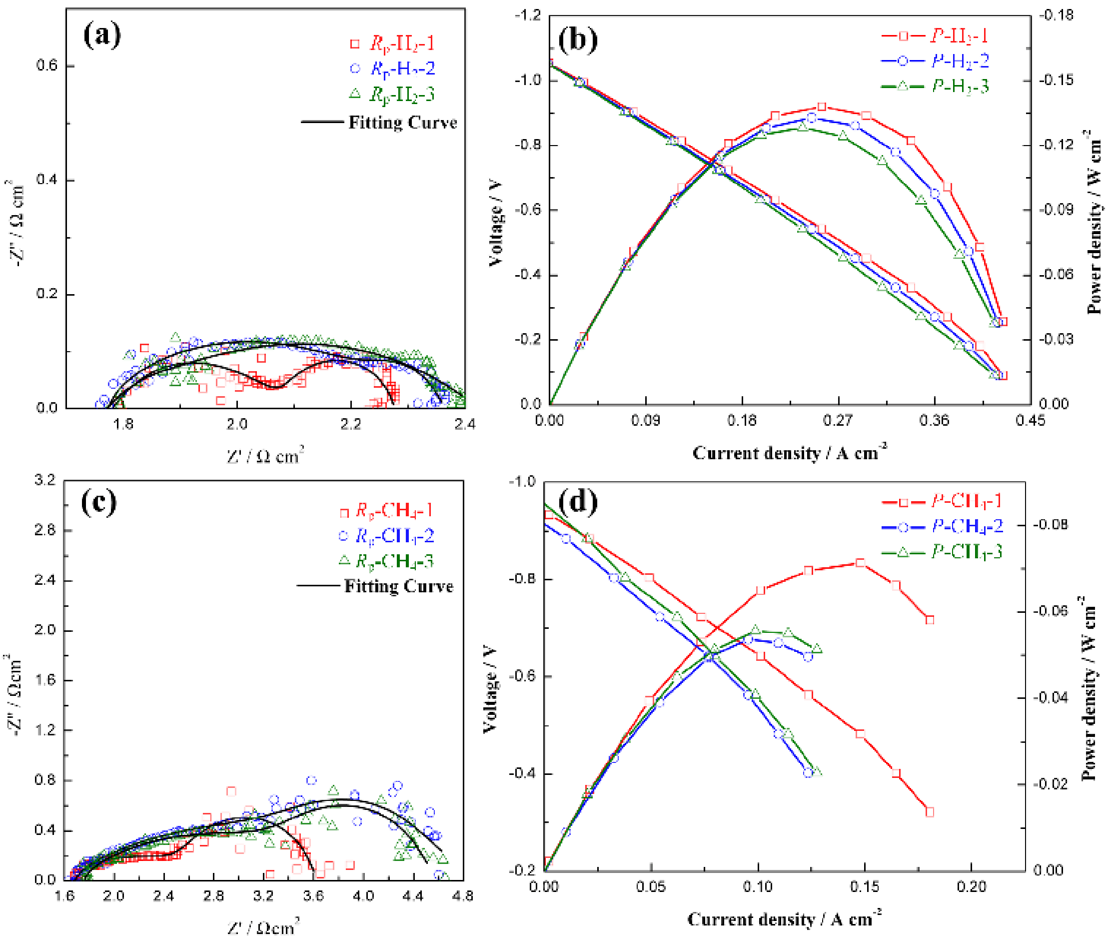

Figure 7. Impedance spectra and fitting results (a,c) and I-V, I-P curves (b,d) of the LST−GDC−Co composite anode measured at 800 °C during the long-term stability test. The fuel gas was humidified H_2 (a,b) or humidified CH_4 (c,d).

Table 1. The obtained polarization resistances (R_p) values and the maximum power density (P_{max}) values when anode fueled with humidified H_2 or CH_4

Fuel gas	R_p (Ω cm^2)			P_{max} (mW cm^{-2})		
97%H_2+3%H_2O	R_p-H_2-1	R_p-H_2-2	R_p-H_2-3	P-H_2-1	P-H_2-2	P-H_2-3
	0.48	0.59	0.61	138.0	132.9	128.2
97%CH_4+3%H_2O	R_p-CH_4-1	R_p-CH_4-2	R_p-CH_4-2	P-CH_4-1	P-CH_4-2	P-CH_4-3
	1.97	2.96	2.85	71.3	53.7	55.5

Fig. 8 shows the cross-section SEM images of the LST−GDC−Co before and after the single cell long-term stability test. The microstructure and porosity of the LST-GDC-Co composite anode did not change significantly after sulfur poisoning for 24 h and carbon deposition for 100 h. Compared with the microstructure of nanofiber-based LST−GDC−Ni composite anodes after sulfur poisoning (see Fig. 4(b)) and after carbon deposition[15], no the obvious adhesion took place and carbon deposition could not be observed in the LST−GDC−Co composite anode after the single cell long-term stability test.

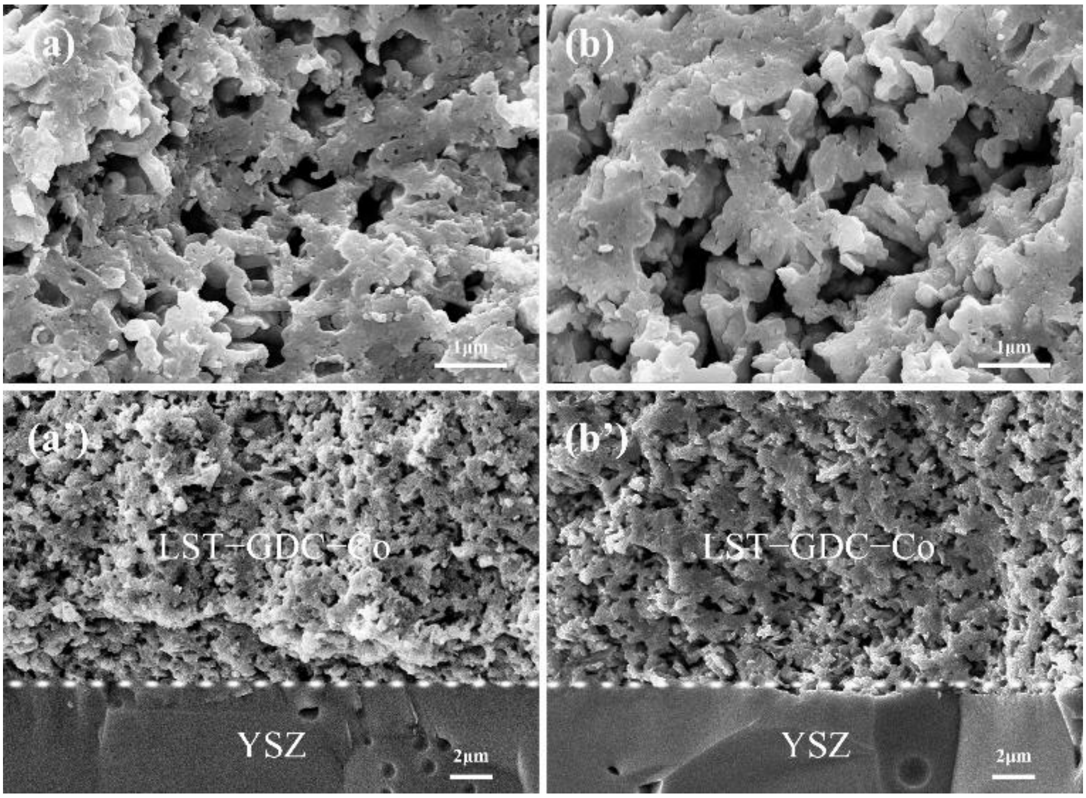

Figure 8. Cross-sectional SEM images of the LST−GDC−Co composite anode before (a,a') and after (b,b') the long-term stability test.

4. CONCLUSIONS

A comparative study on the resistances to sulfur poisoning of the nanofiber-based LST−GDC−Ni and LST−GDC−Co composite anodes was carried out. The electrochemical performance of the LST−GDC−Ni composite anode degraded significantly after sulfur poisoning for 21 h, the R_p increased by 112% and the P_{max} decreased by 33% when fueled with 512 ppm H_2S-H_2 at 800 °C. And we observed obvious adhesion and lower porosity in the LST−GDC−Ni composite anode after sulfur poisoning. However, the LST−GDC−Co composite anode showed a strong resistance to sulfur poisoning. After sulfur poisoning for 24 h, the R_p and P_{max} did not change significantly when fueled with humid H_2, and them changed worsen slightly when fueled with humidied CH_4. The LST−GDC−Co composite anode after sulfur poisoning showed an excellent resistance to carbon depositing, the R_p and P_{max} did not change significantly after carbon depositing for 100 h when fueled with either humidified H_2 or CH_4. Furthermore, the microstructure morphology of the LST−GDC−Co composite anode did not change significantly after 24 h sulfur poisoning and 100 h carbon deposition tests. All told, improved electrochemical performance, greater resistance to sulphur poisoning and carbon deposition, and better microstructure stability when the fuel contained H_2S and CH_4 are the major advantages of LST−GDC−Co composite anodes over LST−GDC−Ni.

ACKNOWLEDGMENTS

This work was supported by the National Natural Science Foundation of China (No. 51502148) and the Natural Science Foundation of Heilongjiang Province, China (No. LH2019E092), and the Fundamental Research Funds in Heilongjiang Provincial Universities (No. 135309349 and No. 135309347).

References

1. W. Wang, C. Su, Y. Wu, R. Ran, Z. Shao, *Chem. Rev.*, 113 (2013) 8104.
2. H. Yokokawa, M. Suzuki, M. Yoda, T. Suto, K. Tomida, K. Hiwatashi, M. Shimazu, A. Kawakami, H. Sumi, M. Ohmori, et al., *Fuel Cells*, 19 (2019) 311.
3. C. M. Grgicak, R. G. Green, J. B. Giorgi, *J. Power Sources*, 179 (2008) 317.
4. D. Jiang, L. Su, L. Ma, N. Yao, X. Xu, H. Tang, X. Li, *Appl. Surf. Sci.*, 256 (2010) 3216.
5. A. Lussier, S. Sofie, J. Dvorak, Y. U. Idzerda, *Int. J. Hydrogen Energy*, 33 (2008) 3945.
6. Z. Cheng, J.-H. Wang, Y. Choi, L. Yang, M. C. Lin, M. Liu, *Energy Environ. Sci.*, 4 (2011) 4380.
7. H. Chen, F. Wang, W. Wang, D. Chen, S. D. Li, Z. Shao, *Appl. Energy*, 179 (2016) 765.
8. J. H. Wang, M. Liu, *Electrochem. commun.*, 9 (2007) 2212.
9. L. Q. Fan, Y. P. Xiong, L. B. Liu, Y. W. Wang, H. Kishimoto, K. Yamaji, T. Horita, *J. Power Sources*, 265 (2014) 125.
10. L. Q. Fan, Y. P. Xiong, Y. W. Wang, H. Kishimoto, K. Yamaji, T. Horita, *J. Power Sources*, 294 (2015) 452.
11. Q. J. Hu, L. Q. Fan, Y. W. Wang, Z. Wang, Y. P. Xiong, *Ceram. Int.*, 43 (2017) 12145.
12. M. Roushanafshar, J. L. Luo, A. L. Vincent, K. T. Chuang, A. R. Sanger, *Int. J. Hydrogen Energy*, 37 (2012) 7762.
13. S.-H. Cui, J.-H. Li, X.-W. Zhou, G.-Y. Wang, J.-L. Luo, K. T. Chuang, Y. Bai, L.-J. Qiao, *J. Mater. Chem. A*, 1 (2013) 9689.
14. R. Mukundan, E. L. Brosha, F. H. Garzon, *Electrochem. Solid-State Lett.*, 7 (2004) A5.
15. Q. Hu, C. Liu, L. Fan, Y. Wang, Y. Xiong, *Electrochim. Acta*, 265 (2018) 1.
16. S. Hui, A. Petric, *Mater. Res. Bull.* 37 (2002) 1215.
17. E. Iglesia, *Appl. Catal. A Gen.* 161 (1997) 59.
18. S. K. Mohapatra, S. U. Sonavane, R. V Jayaram, P. Selvam, *Tetrahedron Lett.*, 43 (2002) 8527.
19. A. Torabi, T. H. Etsell, *J. Power Sources*, 225 (2013) 51.
20. S. Zha, Z. Cheng, M. Liu, *J. Electrochem. Soc.*, 154 (2007) B201.
21. A. Zekri, K. Herbrig, M. Knipper, J. Parisi, T. Plaggenborg, *Fuel Cells*, 17 (2017) 359.
22. L. Yang, L. C. De Jonghe, C. P. Jacobsen, S. J. Visco, *J. Electrochem. Soc.*, 154 (2007) B949.
23. C. H. Bartholomew, P. K. Agrawal, J. R. Katzer, *Adv. Catal.*, 31 (1982) 135.